DOI: 10.31319/2519-2884.46.2025.8
UDC 621.874.7

Kabakov Daniil[1], Candidate of Technical Sciences, Doctoral Candidate
Kabakov Anatoli[2], Candidate of Technical Sciences, Associate Professor of the Department of Mechanical Engineering and Welding Technology
Telipko Leonid[2], Candidate of Technical Sciences, Associate Professor of the Department of Mechanical Engineering and Welding Technology
[1]Ukrainian State University of Science and Technologies
[2]Dniprovsky State Technical University, Kamianske

Кабаков Д.Ю.[1], к.т.н. докторант, ORCID: 0009-0005-6456-0968, e-mail: megafab@live.com
Кабаков А.М.[2], к.т.н., доцент, ORCID:0009-0008-3948-8687, e-mail: kabakovanatoly@gmail.com
Теліпко Л.П.[2], к.т.н., доцент, ORCID: 0000-0003-3165-3920, e-mail: leo46din@gmail.com
[1]Український державний університет науки і технологій
[2]Дніпровський державний технічний університет МОН України, м. Кам'янське

OPTIMIZATION DEVICES FOR VIBRO-PROTECTION AND DYNAMIC LOAD IN LIFTING CRANES

The work is dedicated to studying the effectiveness and feasibility of controlled damping devices installed in the pulley systems of bridge crane lifting mechanisms. It demonstrates the possibility of adjusting the dynamics of non-stationary processes through the application of mathematical modeling methods for certain controlled damping algorithms. A mathematical model of a bridge electromagnetic crane is developed, representing an integrated electromechanical complex. This includes a controlled electric drive, damping device with a corresponding algorithm model, rope, electromagnetic load, and crane metal structure interconnected by elastic links. The study highlights the significant impact of damper parameters on the dynamic and oscillatory processes in the elements of the lifting mechanism and metal structure, depending on the load mass and operating conditions. An automatic damper parameter control system was developed, enabling high vibration damping efficiency across a wide frequency range, improved crane productivity, reduced harmful effects on personnel, and extended mechanism lifespan.

Keywords: *dynamic load; mathematical modeling; damper; crane; parameters; electromagnetic moment.*

Роботу присвячено дослідженню ефективності та доцільності застосування керованих демпфуючих пристроїв, встановлених у системі поліспасту механізму підйому мостових кранів. Показано можливість корекції динаміки нестаціонарних процесів. Це здійснюється шляхом реалізації методів математичного моделювання деяких алгоритмів керованого демпфування. Розроблено математичну модель мостового електромагнітного крана, що представляє єдиний електромеханічний комплекс, який складається з керованого електроприводу, демпфуючого пристрою з відповідною моделлю формування алгоритму управління, каната, електромагніту з вантажем та підкрановими металоконструкціями, які з'єднані між собою пружними зв'язками.. Показано суттєву залежність параметрів амортизатора на характер динамічних та коливальних процесів в елементах механізму підйому та металоконструкції для вантажів різної маси та з урахуванням особливостей умов експлуатації. Розроблено систему автоматичного керування параметрів амортизатора. Це дозволило забезпечити високу ефективність гасіння коливань у великому діапазоні частот та збільшити продуктивність роботи крана, знизити шкідливий вплив моста на обслуговуючий персонал, збільшити термін служби механізмів.

Ключові слова: *динамічне навантаження; розрахункова схема; амортизатор; кран; параметри; електромагнітний момент.*

Problem's Formulation

The calculation of the dynamic load on a crane is considered relevant when lifting a load from the base, as dynamic loads reach their maximum values in this situation. Identifying the parameters that most significantly affect the magnitude of these loads, and developing methods for their reduction, is one of the key problems that greatly influences the reliability of crane operation. The dependence of damping efficiency on the weight of the lifted load and the magnitude of dynamic forces leads to the following objectives:

1. Development and study of a mathematical model of the metal structure and lifting mechanism with a controlled damper, ensuring optimization of the system's dynamic characteristics based on specific operational conditions.
2. Investigation of the influence of controlled damper parameters on the nature of dynamic processes in elastic connections, aiming to develop automatic control algorithms.
3. Creation of an automatic control system for damper parameters, enabling optimization of the damping process for oscillations in the crane's cable and metal structure.

Analysis of recent research and publications

The topic of dynamic loading modes in cranes and the development of methods to reduce dynamic loads, encompassing both structural and technological solutions, has been extensively studied, underscoring the relevance of this issue [1—4]. In [7], it is shown that the dynamic coefficient in the cable significantly depends on the inelastic resistance force of the damper. In [5], theoretical foundations are presented, and differential equations of motion are formulated using Lagrange's second-order equation. In [6], it is demonstrated that the viscosity of magnetorheological fluid (MRF) can be altered by varying its physical and mechanic properties.

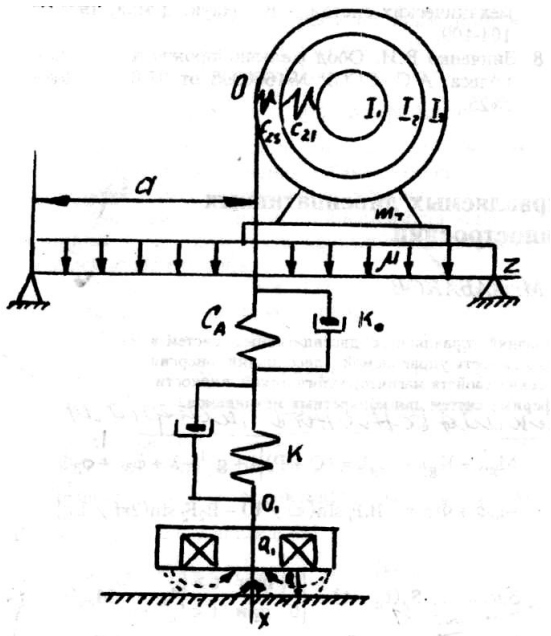

Fig. 1. Calculation model of the dynamic system of the bridge electromagnetic crane

Formulation of the study purpose

The studies mentioned above highlight the relevance of developing dynamic load modes for cranes and methods to reduce their dynamic loading. The aim of this article is to develop and investigate a mathematical model of the lifting mechanism with a controlled damper that ensures the optimization of the system's dynamic characteristics based on specific operational conditions

Presenting main material

To study the influence of damper parameters on the dynamics of lifting machines, a calculation model was created (Fig. 1), and the system of differential equations of motion for the mechanical part of the system during load lifting was derived using Lagrange's second-order equation. Considering the oscillation modes of the beam ($j = 2$):

$$M_{MT}(t) = (3/2)p\omega_0(K_r/x_e\sigma)\times$$
$$\times(\psi_{\alpha r}\psi_{\beta s} - \psi_{\alpha s}\psi_{\beta r});$$
$$\dot{\psi}_{\alpha s} = u_{\alpha s} - \omega_0\alpha_s'\psi_{\alpha s} + \omega_0\alpha_s'K_r\psi_{\alpha r};$$
$$\dot{\psi}_{\beta s} = u_{\beta s} - \omega_0\alpha_s'\psi_{\beta s} + \omega_0\alpha_s'K_r\psi_{\beta s};$$
$$\dot{\psi}_{\beta r} = \alpha_r'\omega_0[1 - (1-K)S_g(t_n - t)]\times$$
$$\times(\psi_{\beta s}K_s - \psi_{\beta r}) + \dot{\phi}_1\psi_{\alpha r};$$
$$\dot{\psi}_{\alpha r} = \alpha_r'\omega_0[1 - (1-K)S_g(t_n - t)](\psi_{\alpha s}K_s - \psi_{\alpha r}) - \dot{\phi}_1\psi_{\beta s};$$
$$I_1\ddot{\phi}_1 + C_{12}(\phi_1 - \phi_2) = M_{дв}(t);$$
$$I_2\ddot{\phi}_2 + C_{12}(\phi_1 - \phi_2) + C_{23}(\phi_2 - \phi_3) = 0;$$
$$I_3\ddot{\phi}_3 + C_{23}(\phi_2 - \phi_3) = -(Q+P)\times$$
$$\times\{1 + g^{-1}[\ddot{\phi}_3 r + \dot{\phi}_3\dot{\Phi}r - l_0\ddot{\Phi}] + \phi_3 r\ddot{\Phi} - B_1\ddot{F}_1\sin(\pi a/b) - B_2\ddot{F}_2\sin(2\pi a/b) - \ddot{\lambda}\}r;$$

$$(Q+P)(l_0-\varphi_3 r)\ddot{\Phi}+[\xi g-\dot{\varphi}_3 r(Q+P)]\dot{\Phi}+E_k S_k \Phi g-(Q+P)\times$$
$$\times\left[r\ddot{\varphi}_3+g-B_1\ddot{F}_1\sin(\pi a/b)-B_2\ddot{F}_2\sin(2\pi a/b)-\ddot{\lambda}\right];$$
$$\ddot{F}_1+\omega_1^2\left(1{,}01\cdot 10^{-2}\dot{F}\omega+F_1\right)=$$
$$=(Q+P)\left[1+g^{-1}\left(\ddot{\phi}_3 r+\dot{\phi}_3\dot{\Phi}r-l_0\ddot{\Phi}+\ddot{\Phi}\phi_3-\ddot{\lambda}\right)\right]B_1\,sin(\pi a/b)-$$
$$-[(Q+P)/g+m_T]\left[B_1^2\ddot{F}_1\,sin^2(\pi a/b)+B_1B_2\ddot{F}_2\,sin(2\pi a/b)\right];$$
$$\ddot{F}_2+\omega_2^2\left(1{,}01\cdot 10^{-2}\ddot{F}_2\omega_2+F_2\right)=$$
$$=(Q+P)\left[1+g^{-1}\left(\ddot{\phi}_3 r+\dot{\phi}_3\dot{\Phi}r-l_0\ddot{\Phi}+\ddot{\Phi}\phi_3 r-\ddot{\lambda}\right)\right]B_2\,sin(2\pi a/b)-$$
$$-[(Q+P)/g+m_m]\left[B_2^2\ddot{F}_2\,sin^2(2\pi a/b)+B_1B_2\ddot{F}_2\,sin(\pi a/b)\,sin(2\pi a/b)\right];$$
$$M_D\ddot{\lambda}+K_d\dot{\lambda}+C_Д\lambda=$$
$$=(Q+P)\left\{1+g^{-1}\left[-\ddot{\lambda}+\ddot{\phi}_3 r+\dot{\phi}_3\dot{\Phi}r-l_0\ddot{\Phi}+\ddot{\Phi}\phi_3 r-B_1\ddot{F}_1\,sin(\pi a/b)-B_2\ddot{F}_2\,sin(2\pi a/b)\right]\right\}.$$

Here $S_g(t_n-t)=\begin{cases}1 when \geq t_n;\\ 0\ when < t_n;\end{cases}$ $M_{MT}(t)$ — electromagnetic torque of the motor;

t_n — time for switching resistance levels in the rotor circuit;

$K=1+R_Д/R_r$ — multiplicity of the active resistance in the rotor circuit;

R_s, R_r, Xs, X_r— active and inductive resistances of the stator and rotor windings;

$\psi_{\alpha s}, \psi_{\beta s}, \psi_{\alpha r}, \psi_{\beta r}$— magnetic flux linkage of the stator and rotor windings;

X_0 — inductive resistance due to mutual induction between the stator and rotor windings;

p — number of pole pairs in the motor

ω_0 — angular frequency of rotation of the magnetic field;

$u_{\alpha s}, u_{\beta s}$ — phase voltages of the stator, aligned with axes α, β;

$\alpha_s^{'}, \alpha_r^{'}, K_r, K_s$— constants of the motor;

$I_1, \phi_1, I_2, \phi_2, I_3, \phi_3$ — moments of inertia and rotation angles of the motor rotor, reducer, and drum;

C_{12}, C_{23} — torsional stiffness of elastic links between the motor rotor and reducer, and between the reducer and drum;

$E_к, S_к$— elastic modulus and cross-sectional area of the cable;

Q — mass of the loaded cargo;

$m_т$ — mass of the trolley;

b— crane span;

a— position of the trolley along the crane span;

r — radius of the drum;

l_0 — initial length of the cable;

Φ — unknown function of time representing absolute extension of the cable section;

ξ — coefficient characterizing the degree of attenuation of dynamic forces in the cable;

ω_j — eigenvalues of circular vibration frequencies of the beam;

B_j — constants determined by normal orthogonality conditions;

F_j — unknown time functions for determining beam deflection;

P — force of interaction between the electromagnet and the metal base;

$C_д$ — total stiffness of the damper springs;

λ — displacement of the damper piston;

M_D — mass of the damper;

$K_d=\varepsilon\eta lS^2/(\pi d^4 n)$ — damper constant determined by the force of viscous friction during fluid throttling

ε — dimensionless coefficient determined by throttling conditions;

η — dynamic viscosity of the damper's working fluid;

d,l,n,S — Diameter, length, number of throttle holes, and piston area of the damper;

g — acceleration due to gravity.

In theequations of motion, represented by the system of differential equations, the reduced electromagnetic moment of the engine $M_{MT}(t)$ is included. Neglecting electromagnetic transitional

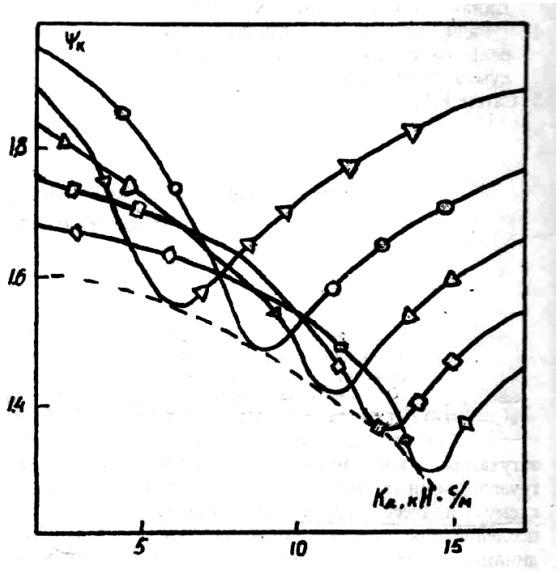

Fig. 2. Dependency of the dynamic coefficient in the cable on the damper constant $\psi_к$for loads weighing Q = 1.5 tons (∇); 2.5 tons (O); 3.5 tons (Δ); 4.5 tons (□); 5.5 tons (◊)

processes leads to incorrect assessments of efforts in the elastic elements of the lifting mechanism and crane structures. Additionally, the uniform distribution of the metal structure's mass across the crane span is considered, along with the elasticity of key connections. For cranes operating with electromagnets, the magnetization effect of the load to the metal base is also taken into account.

The system (1) was solved numerically. In Fig. 2, graphs show the dependence of the dynamic coefficient in the cable on the damper constant ψ_k for loads of different weights. As evident from the family of graphs, the dynamic coefficient significantly depends on the damper constant $K_d$for various load weights. Furthermore, there is an optimal value of the damper constant for a specific load weight at which dynamic cable loads are minimal (indicated by the dashed line in Fig. 2). Thus, for the efficient operation of the damper, its parameters must be adjusted based on the weight of the lifted load. The damper control process should be automatic and primarily carried out through electrical interaction affecting its physical parameters, due to the high oscillation frequency of the mechanical system.

The force of interaction between the electromagnet and the metal base P is determined by the Maxwell formula.

$$P = \frac{I^2 n^2 G^2}{2\mu_0 S},$$

where $\mu_0 = 4\pi \cdot 10^{-7}$H/m — absolute magnetic permeability of vacuum; S — contact area between the electromagnet and the load; I_n — magnetizing force of the coil; G — total magnetic conductivity.

On Fig. 3, the change in the gravitational force depending on the gap for round and rectangular load electromagnets (load — steel plate) is presented.

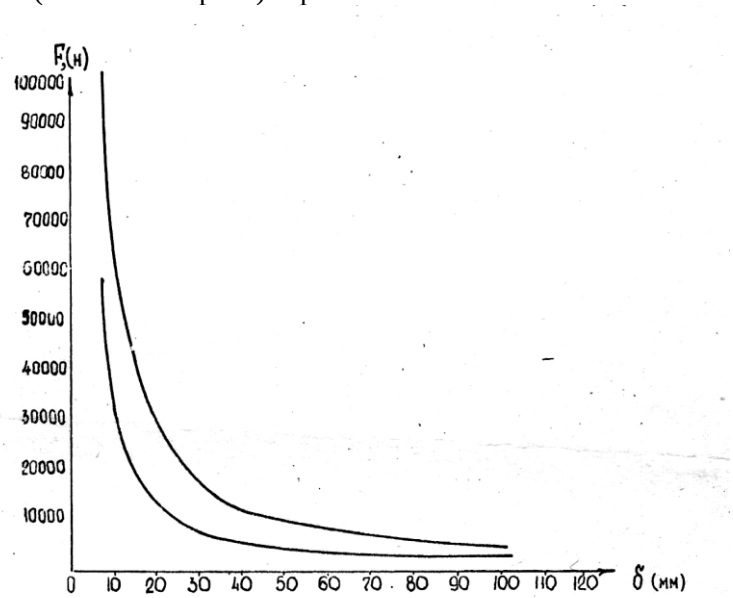

Fig. 3. Graph of the dependency of gravitational force on the gap

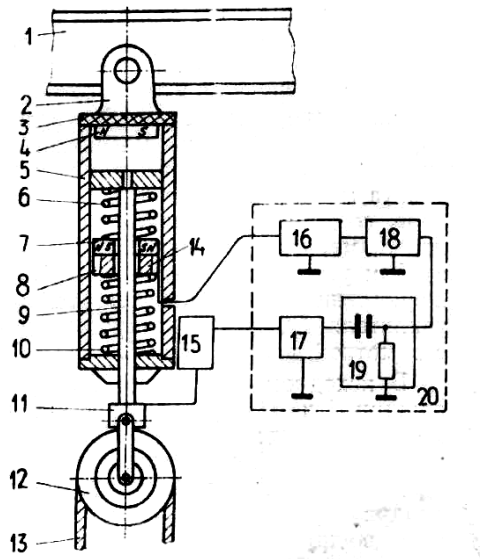

Fig. 4. Damper with controlled correction of the stiffness of elastic elements

The stiffness management system of the elastic elements, consisting of a controlled damper, an oscillation velocity sensor, and a control signal formation unit, is shown in Fig. 4.

The controlled damper has a housing 3 inside which the upper 6 and lower 10 springs are arranged one above the other, with the stiffness of spring 10 exceeding that of spring 6. A permanent magnet 4 is installed at the top of housing 3. Between the springs 6 and 10, a permanent magnet with an opening 7 and the lower piston 14 are located, which can move along the rod 9. Along the periphery of piston 14, excitation windings 8 are placed in grooves, connected to the velocity sensor 15 through a signal forming unit 20. The rod 9 is connected at one end to the upper piston 5 and at the other end to the pulley bracket 12 of the cable-driven system. The velocity sensor 15 is directly mounted on the housing 3 and connected to the rod 9 via a hinge 11, enabling the measurement of the relative velocity of the rod 9 with respect to housing 3. The housing, rod, and pistons are made of magnetic material. The cavity of the housing 3 is filled with magnetorheological fluid (MRF), which changes its viscosity under the magnetic field created by the permanent magnets 4 and 7 and the excitation winding 8.

In the initial state (no load), pistons 5 and 14, under the action of springs 6 and 10, are in their extreme positions, with no current in the excitation winding 8. During load lifting, the upper piston 5 compresses spring 6 and moves downward relative to the housing cylinder 3. The MRF flows through the annular gaps between the internal walls of the housing cylinder 3 and pistons 5 and 14, with the hydraulic resistance of these gaps determining the damping force and piston velocity.

Damper control involves changing the hydraulic resistance by creating a radial magnetic field in the gaps. As spring 6 compresses, the distance between piston 5 and magnet 7 decreases, resulting in increased magnetic field induction in the annular gap between piston 5 and housing cylinder 3. This raises the viscosity of the MRF, leading to additional energy dissipation during oscillations. The permanent magnet 4 located at the top of the housing 3 provides further damping during upward piston movement by altering the throttling conditions of the MRF in the gap between the piston and housing. As a result, the total energy dissipation over a vibration cycle increases significantly

Since the stiffness of springs 6 and 10 differs, the displacement of the upper piston 5 will be greater than that of the lower piston 14. During the reverse motion of components 5, 6, 7, 8, 9, 10, 12, 13, 14, the suspension of the velocity sensor 15 transmits power to the excitation winding 8 via the signal forming unit 20. In this case, a magnetic field of sufficient intensity is induced in the gap between piston 14 and the inner cylindrical surface of housing 3. This creates a hydraulic resistance in the lower annular gap that prevents piston 14 from moving relative to housing 3. Consequently, the stiffness of the elastic elements of the damper is determined solely by the stiffness of the upper spring 6.

Velocity sensor 15, which records the movement of rod 9 relative to housing 3, generates an electrical signal proportional to the relative velocity between the rod and housing, i.e., the oscillation velocity v:

$$u_{\partial} = K_1 dx/dt = Kv,$$

where $K$is the sensitivity coefficient of the sensor.

In the control signal formation unit 20, the initial electrical signal is limited by the amplifier-limiter 17, then differentiated by the RC chain 19, whose time constant is chosen based on the oscillations occurring:

$$u_1 = K_1 u_{\partial} + RCdu_c/dt \approx K_1\, RCdu_0/dt,$$

where $K_1$is the amplification coefficient of the amplifier-limiter 17.

The differentiated signal determines the phase of movement of rod 9, as the derivative of the velocity changes sign in this case. This signal, with a steep front and exponential decrease in tension $u_2 = u_0\, exp(-t/RC)$, where $u_0$is the level of signal restriction arising at the moment of rod 9 direction reversal, passes through the buffer amplifier to exclude the influence of subsequent blocks on the operation of the differentiating circuit. Then, the power amplifier 16 induces current in the excitation winding:

$$i = u_b/R_\partial = K_2 u_0\, exp(-t/RC)/R_\partial.$$

Here K_2s the generalized transfer coefficient of the buffer amplifier and power amplifier, also characterized by an exponential decrease over time and an initial level sufficient to completely block piston 14.When piston 14 is fixed in place, the initially less stiff spring 6 gradually returns to its original position due to throttling of the MRF in the annular gap between housing 3 and piston 5. Subsequently, as the exponential decay in excitation winding current progresses, the previously blocked spring 10 gradually releases. Part of its energy is transferred to piston 5 and rod 9 via additional compression of spring 6, which, in turn, reduces the load during the reverse stroke of the rod. Thus, the presence of controlled blocking of piston 14 allows efficient damping of rebound energy from the spring, which is released in two stages, thereby contributing to an overall reduction in dynamic loads.

Conclusions

1. Control of the damper through the stiffness of its elastic elements C_g allows achieving a progressive characteristic of resistance forces, ensuring high efficiency in vibration damping over a broader frequency range while simultaneously adjusting the damper parameters.
2. Calculations provided the initial data for designing controlled dampers.
3. Operational experience with these devices has demonstrated that the use of shock absorbers has increased crane productivity.

References

[1] Ivanchenko F.K. (2008). Pidiomno-transportni mashyny: Navchalnyi posibnyk. [Lifting and transport machines: textbook]. Kyiv: Vyshcha shkola, 413 p. [in Ukrainian].

[2] Bondariev O.I. et al. (2009). Pidiomno-transportni mashyny: Rozrakhunky pidiimalno-transportuvalnykh mashyn. [Lifting and transport machines: Calculations of lifting and transporting machines]. Kyiv: Vyshcha shkola, 734 p. [in Ukrainian].

[3] Hryhorov O.V., Okun A.O. (2017). Udoskonalennia matematychnoi modeli rukhu dlia zadachi keruvannia pidiomno-transportnymy mashynamy. [Improvement of the mathematical model of movement for the problem of control of lifting and transport machines]. Avtomobilnyi transport, Kyiv, 127 p. [in Ukrainian].

[4] Ohurtsov A.P. et al. (2002). Diahnostyka, dynamika, nadiinist pidiomno-transportnykh system. [Diagnostics, dynamics, reliability of lifting and transport systems]. Dnipropetrovsk: Systemni tekhnolohii, 368 p. [in Ukrainian].

[5] Pavlovskyi M.A. (2022). Teoretychna mekhanika. [Theoretical mechanics]. Kyiv: Tekhnika, 512 p. [in Ukrainian].

[6] Kabakov A.M., Telipko L.P. (2024). Matematychne modeliuvannia krana z vantazhem i kerovanymy prystroiamy vibrozakhystu. [Mathematical modeling of a crane with a load and controlled vibration protection devices]. European congress of scientific achievements. Proceedings of the 1st International Scientific and Practical Conference. Barca Academy Publishing, Barcelona, Spain, pp. 91–98. [in Ukrainian].

[7] Doslidzhennia dynamiky, mitsnosti i tekhnolohichnosti mekhanichnykh system. [Research on dynamics, strength, and manufacturability of mechanical systems]. (2017). Monograph. Kamianske: DDTU, 182 p. [in Ukrainian].

ПРИСТРОЇ ОПТИМІЗАЦІЇ ВІБРОЗАХИСТУ ТА ДИНАМІЧНОГО НАВАНТАЖЕННЯ ВАНТАЖОПІДЙОМНИХ КРАНІВ

Реферат

У статті розроблена математична модель механізму підйому мостового електромагнітного крана як єдиного електромеханічного комплексу, що включає в себе керований електропривід, амортизатор з керованою корекцією жорсткості пружинних елементів, канат, електромагніт з вантажем та підкранова металоконструкція, з'єднаних між собою пругкими зв'язками. Досліджено вплив параметрів амортизатора на характер динамічних навантажень і коливальних процесів в пругких елементах механізму підйому та металоконструкції. Показана їх суттєва залежність від параметрів амортизатора для вантажів різної маси. Розроблена система управління жорсткості пружинних елементів, що складається з керованого амортизатора, датчика швидкості коливань та блоку формування сигналу управління, що дозволило отримати прогресивну характеристику сил опору і забезпечило ефективність гасіння коливань.

Література

1. Іванченко Ф.К. Підйомно-транспортні машини. К.: Вища школа. 2008. 413 с.
2. Підйомно-транспортні машини: Розрахунки підіймально-транспортувальних машин / Бондарєв О.І. та ін. К.: Вища школа. 2009. 734 с.
3. Григоров О.В., Окунь А.О. Удосконалення математичної моделі руху. Автомобільний транспорт для задачі керування підйомно-транспортних машин. К. 2017. 127 с.
4. Огурцов А.П. та інші. Діагностика, динаміка, надійність підйомно-транспортних систем. Дніпропетровськ: Системні технології. 2002. 368 с.
5. Павловський М.А. Теоретична механіка, К.: Техніка. 2022. 512 с.
6. Кабаков А.М., Теліпко Л.П. Математичне моделювання крана з вантажем і керованими пристроями віброзахисту // European congress of scientific achievements. Proceedings of the lst International scientific and practical conference. Barca Academy Publishing. Barcelona, Spain. 2024. С. 91–98.
7. Дослідження динаміки, міцності і технологічності механічних систем. Монографія. Кам’янське. ДДТУ. 2017. 182 с.

Надійшла до редколегії 31.03.2025